Three-dimensional Photoelastic Study of the Load-carrying Capacity/Face Width Ratio of Wildhaber–Novikov Gears for Automotive Applications

Three-dimensional photoelastic technique has been used for the analysis of contact and bending stresses in Wildhaber–Novikov circular-arc helical gears. Feasibility of using helix angles up to 40 deg for automotive applications has been studied

by K. Lingaiah and K. Ramachandra

ABSTRACT—Wildhaber-Novikov gears are becoming more and more popular for heavy load applications. They have been tried as speed-reducing gears, in spite of heavy noise generation, in aircraft jet engines, marine engines and agricultural machinery. These circular-arc gears, though stronger than involute gears, have the disadvantage of needing larger face width. Axial face width required can be minimized only at the expense of load-carrying capacity. This is not a serious disadvantage with stationary engines. But in the case of automotive applications, this fact limits the load-carrying capacity of Wildhaber-Novikov gears, since space problem is very critical in these applications and large face widths, therefore, cannot be used for such gear-reduction units. The face width is determined by the helix angle and, therefore, a thorough investigation of the dependence of the load-carrying capacity on helix angle is necessary, if these special types of gears have to make headway into the automotive field.

In this experimental investigation, three-dimensional photoelastic technique has been employed to study the load-carrying capacity/face width ratio. Three-dimensional gear models made of epoxy castings (Araldite B) were loaded in a specially built gear-loading fixture and were stress frozen. Gear cutters of Wildhaber-Novikov gears developed at the laboratory were used for the preparation of these three-dimensional gear models. The stress-frozen models were analyzed using the conventional slicing technique to study the contact and bending-stress distribution along the face width. The load-carrying capacity in terms of contact stress and bending stress has been studied for different face widths and helix angles.

Twenty-deg pressure angle, 14-mm module gears of all-addendum type of Wildhaber-Novikov gears with different helix angles up to 40 deg were tested. The helical-overlap ratio used was 1.0. The conventional profile parameters were employed for the manufacture of gear cutters of end-mill type.

The decrease in contact and bending strength with increase in the helix angle or decrease in the face width, as obtained from this photoelastic method of stress analysis has been compared with existing theoretical results.

K. Lingaiah is Professor of Mechanical Engineering (Post-Graduate Studies) and Head and Principal; K. Ramachandra is Lecturer in Mechanical Engineering (Post-Graduate Studies) University Visvesvaraya College of Engineering, Bangalore University, Bangalore-560001, India.

Paper was presented at 1974 SESA Spring Meeting held in Detroit, MI on May 14-17.

List of Symbols

a' = semimajor axis of the contact ellipse, mm
b = face width of gear, mm
b' = semiminor axis of the contact ellipse, mm
C_1, C_2 = constants
d_1' = pitch diameter of the pinion, mm
d_2' = pitch diameter of the wheel, mm
E = Young's modulus of the gear material, Pa
f_σ = stress-fringe coefficient of the material, N/m-fringe
h_{a1} = addendum height of the pinion, mm
h_{f2} = dedendum height of the wheel, mm
i = gear ratio
k = material constant
k_h = helical-overlap ratio
m = module, mm
n_c = fringe order at the contact point
n_f = fringe order at the root fillet
r_{fi} = fillet radius of the pinion tooth
s_1 = tooth thickness of the pinion tooth, mm
s_2 = tooth thickness of the wheel tooth, mm
W_n = applied normal load on the gear teeth, N
x, y = constants defining the semimajor and semiminor axes of the contact ellipse
z_1 = number of teeth on the pinion
z_2 = number of teeth on the wheel
α = pressure angle, deg
β = helix angle, deg
ϵ_1, ϵ_2 = sum and difference of the ratio of the quadratic equation defining the contact area
θ = angle dependent on ϵ_1 and ϵ_2, deg
λ = constant
ν = Poisson's ratio of the material of the gear
ϱ_1 = profile radius of the pinion tooth, mm
ϱ_2 = profile radius of the wheel tooth, mm
σ_c = contact stress, Pa
ϕ = constant

Introduction

With the widely discussed and confirmed fact that unhardened Wildhaber-Novikov circular arc gears (Fig. 1) are at least 3.5 times stronger than involute gears of same module and helix angle,[1-5] it is no wonder that they have been tried successfully as gainful substitutes for involute gears in automotive applications such as vertical-take-off

(VTO) aircrafts, helicopters, marine engines, agricultural machinery and even in industrial power transmissions such as hoists, cement mill drives.[6-10] These high-strength gear teeth, with proper hardening and heat treatment, result in light-weight gears and gear boxes and this is an essential requirement in automotive gear boxes. However, the kinematic requirements of these gears make it imperative to use larger face width as compared to the involute system, in which the required face width is dictated only by the transmitted load, for a particular profile geometry. The face width required for Wildhaber-Novikov gears, for constant-velocity-ratio transmission, is given by the relation,

$$b = k_h \frac{\pi m}{\tan \beta} \tag{1}$$

The design criterion for these gears could be either the contact stress or the bending stress, depending upon the profile chosen, material of the gear and the type of application. Much, however, depends upon the profile geometry—the profile radii of the contacting teeth, the thickness of the teeth, the height of the teeth, fillet radii, helix angle and pressure angle. With so many variables, it is difficult to get the exact relation between the load-carrying capacity and face width.

The existing theoretical predictions of contact and bending stress in Wildhaber-Novikov gears have several approximations. Based on two-dimensional analysis—without taking the effect of the curvature of helical teeth and difference in profile radii, $\Delta\varrho$, into consideration—it is reported that the contact and bending stress of Wildhaber-Novikov gears increase with the increase in helix angle.[1] The classical bending-stress theories, which treat the gear teeth as thin or thick cantilever plates, are still approximations, since they do not take into account the effect of shear deformations due to transverse shear loads, particularly in the case of Wildhaber-Novikov gear teeth, as the teeth are much stubbier than involute-gear teeth. Two-dimensional analysis of gear teeth as cantilever plate also implies that the effect of curvature of helical-gear teeth is not taken into consideration in evaluating the bending stresses. Theoretical prediction of contact stress has also been simplified by assuming $\Delta\varrho$ to be zero, and this has a great influence on the area of contact and magnitude of the contact stress predicted.[11] To avoid these basic approximations in analyzing the contact and bending stress, this experimental investigation was taken up, since three-dimensional photoelastic technique readily gives the stress distribution along the face width of the gear teeth.

Most of the automotive gears employ high helix angles, as compared with industrial gears, since the cost of manufacture and assembly, in the case of lower-helix-angle gears, is higher and these low-helix-angle gears are more prone to center-distance and profile errors. For the standard modules and diameters of gear wheels employed, helix angles less than 20 deg would result in too large a face width for automotive applications. For this reason, the load-carrying capacity of Wildhaber-Novikov helical gears, with helix angle ranging from 20 to 40 deg, is studied.

Experimental Setup

Three-dimensional photoelastic models of Wildhaber-Novikov helical gears which were prepared from epoxy material, Araldite B, have equal number of teeth on the pinion and wheel. The standard dimensions of the profiles used are given in Table 1.

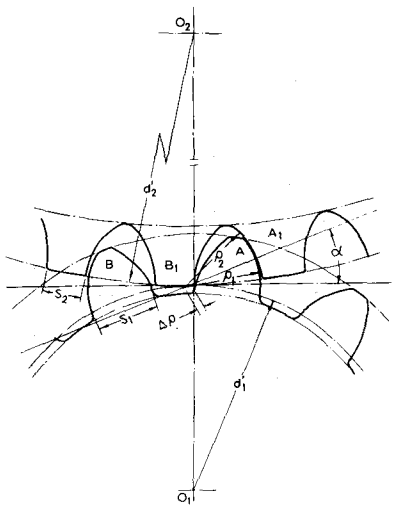

Fig. 1—All-addendum type of Wildhaber-Novikov gear

The photoelastic models of Wildhaber-Novikov gears were machined using end-mill type of form-milling cutters indigenously developed at the authors' laboratory. Two separate form-milling cutters—one for the convex profile and the other for concave profile—were used for each helix angle, since the normal section changes with each helix angle.

The photoelastic models were stress frozen after being loaded in a specially built gear-loading fixture (Fig. 2). The wheel segment was held rigidly without rotation or translation in two journals which can be moved along the guideways, in the frame of the fixture and locked at the required distance from the pinion shaft. The pinion shaft was supported in two ball bearings and was rotated by a balanced loading lever, at one end of which a load was applied. The body of the loading fixture was made of

TABLE 1—DIMENSIONS OF THE WILDHABER-NOVIKOV GEAR MODELS

Module, m	= 14 mm
Pressure angle, α	= 20 deg
Gear ratio, i	= 1.0
Number of teeth, z	= 18
Profile radius, ϱ_1	= 21.00 mm
Profile radius, ϱ_2	= 23.10 mm
Tooth thickness, s_1	= 25.90 mm
Tooth thickness, s_2	= 17.26 mm
Addendum, h_{a1}	= 16.10 mm
Dedendum, h_{f2}	= 18.20 mm
Fillet radius, r_{f1}	= 4.00 mm
Helical-overlap ratio, k_h	= 1.0

Helix Angle β, deg	Face Width b, mm
20	120.00
25	94.00
30	76.20
35	62.60
40	52.10

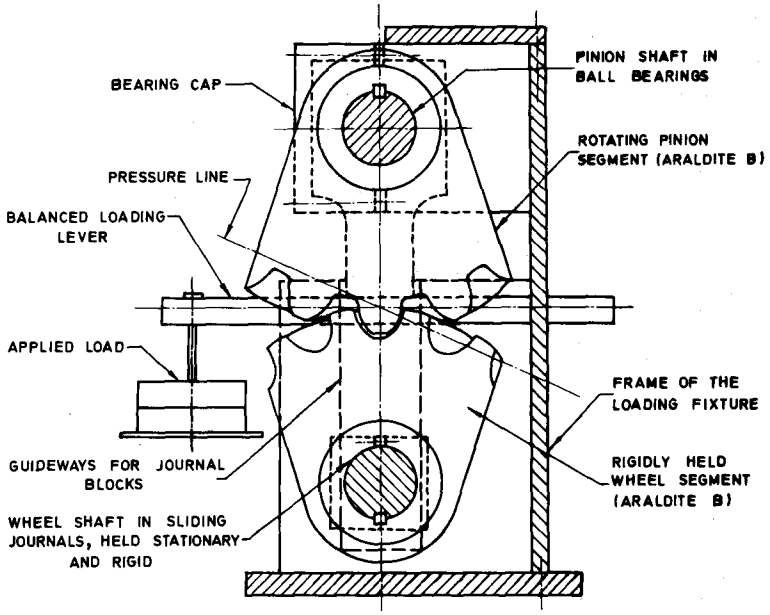

Fig. 2—Details of gear-loading fixture

mild steel. The loading fixture had provisions for changing the center distance between the gear shafts and also the position of the point of contact along the meshing teeth, in the axial direction.

Stress Freezing and Slicing

Helical-overlap ratio equal to 1.0 was used for these Wildhaber-Novikov gears under investigation. The critical stresses occur, therefore, when the contact point changes from one tooth to the next. The angular positions of the pinion and wheel were adjusted to obtain this kinematic arrangement. The wheel was locked up in this position and the torque was applied through the pinion. The load applied on the loading lever in each case, depending upon the face width and the rigidity of the teeth, was just

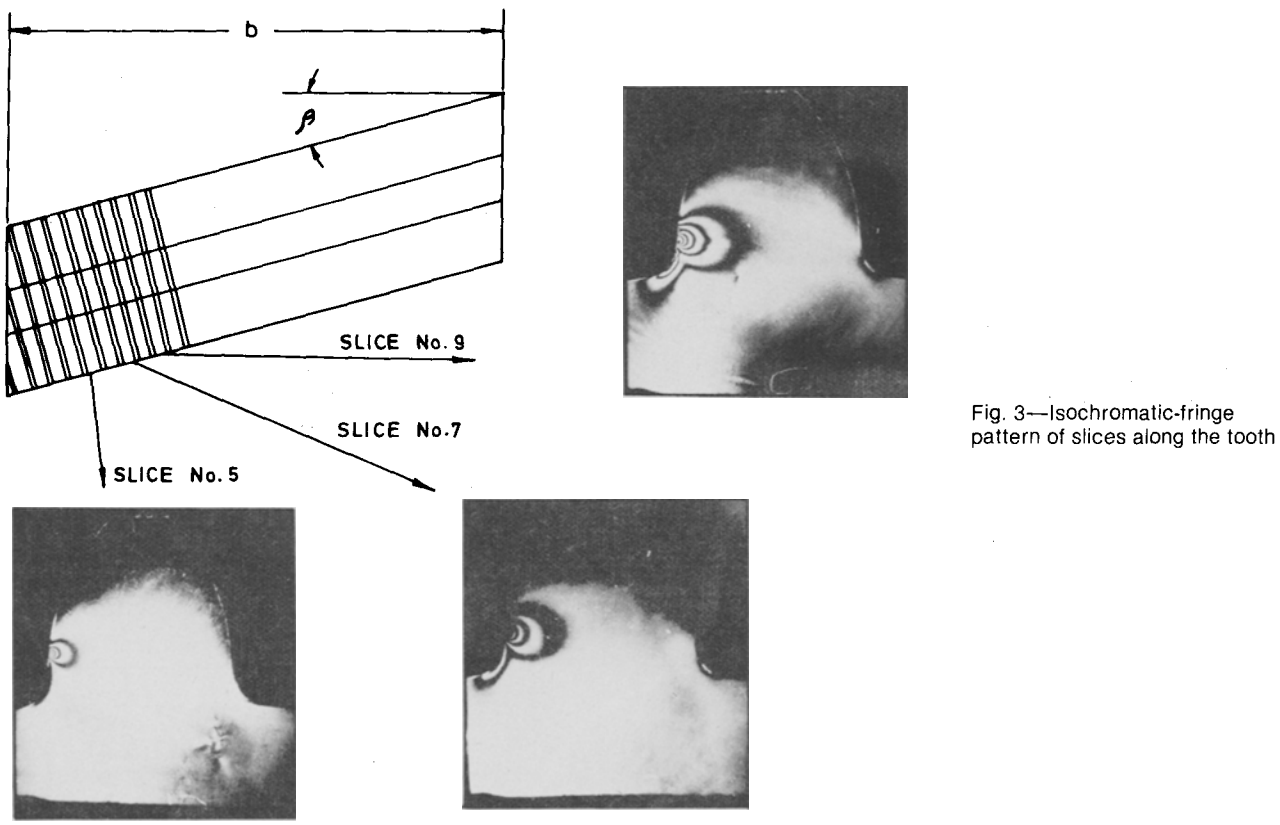

Fig. 3—Isochromatic-fringe pattern of slices along the tooth

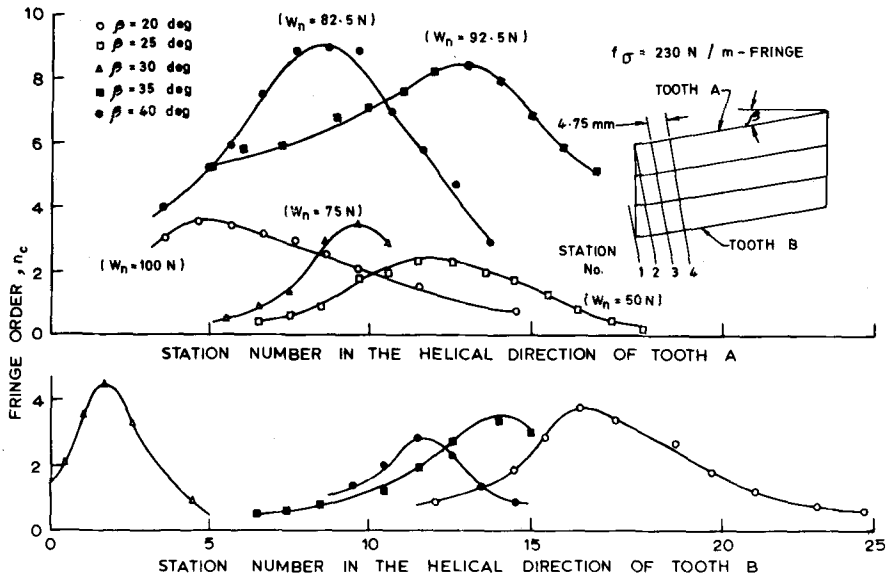

Fig. 4—Contact-stress distribution in pinion teeth

sufficient to take up the backlash between the profiles, at the critical temperature of the photoelastic material, since the tooth deflection in each case depends upon the face width of the tooth, the tooth profile and the load applied. The photoelastic models were stress frozen in a photoelastic oven with a minimum soaking period of 72 h and a maximum cooling rate of 1 deg/h, depending upon the dimensions of the models. The interest in this analysis being the maximum surface stresses and their distribution along the face width for different helix angles, normal slices were taken along the meshing teeth, using a rotary-slitting saw. The normal slices were analyzed for maximum contact and bending stresses using the isochromatic-fringe patterns obtained. Typical isochromatic-fringe patterns of the slices from 25-deg-helix-angle convex-profiled pinion tooth is shown in Fig. 3. An immersion fluid, tricricylphosphate, was used for the analysis of the slices up to 2.75 mm in thickness.

Experimental Results

The surface stresses at the flanks and fillets of the gear teeth have been analyzed and reported, as the aim of the paper is only to make a comparative study of the load-carrying capacity of Wildhaber-Novikov gears at higher helix angles.

The maximum flank stress along the tooth helix is plotted for convex-profiled all-addendum pinion teeth (Fig. 4). Figure 5 shows the maximum flank stress in the concave-profiled all-dedendum wheel teeth. It is seen that, excepting in the case of 25-deg helix angle, there is double contact between the adjacent teeth owing to the deflection of the teeth at the critical temperature of the photoelastic material. Excepting the case of 20-deg helix angle, there is unequal load sharing between adjacent teeth. Figures 4 and 5 indicate the severity of the contact stress at higher helix angles.

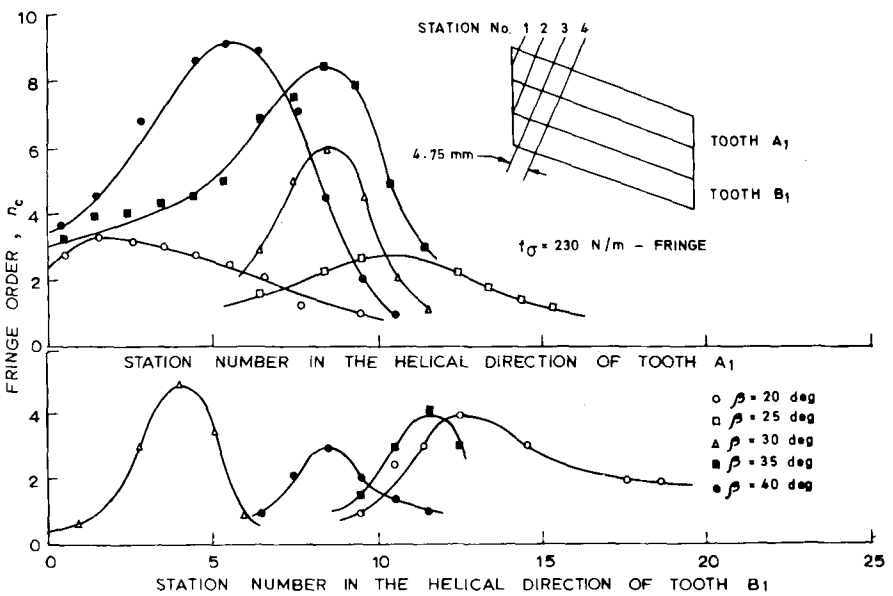

Fig. 5—Contact-stress distribution in wheel teeth

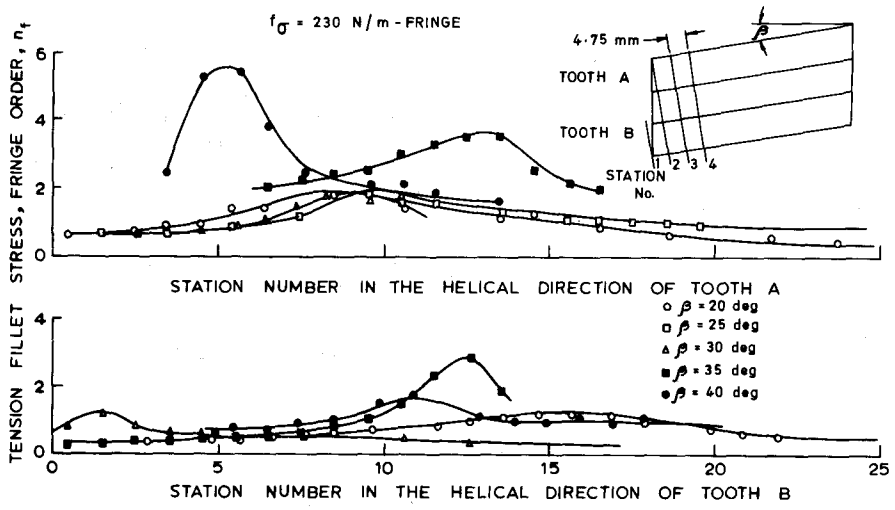

Fig. 6—Bending stress (tension fillet) in convex-profiled teeth

The fillet-stress variation at the tension fillet of the pinion teeth is given in Fig. 6. A more-uniform stress distribution in the case of lower-helix-angle gears is evident from this figure, in contrast to the highly localized bending stresses as in the case of 35- and 40-deg-helix-angle gears. The stiffness of the curved teeth at higher helix angle will not be sufficient to take up the higher localized bending loads.

Since the load transmitted is shared by two pairs of teeth, the reciprocal of the total area under the stress curves for any pair of adjacent teeth gives the load-carrying capacity of gear teeth of that particular helix angle. The total areas under the contact and bending-stress curves are plotted (Fig. 7) against the face width which is related to the helix angle. It is seen that the areas under both contact and bending stress increase with decrease in the face width indicating stronger tooth form and more favorable load distribution at lower helix angles. The maximum fringe orders at the tooth flank and tooth fillet are also plotted for different helix angles (Fig. 8). The variation of contact stress obtained from this experimental investigation agrees with that obtained theoretically for Araldite B, under critical temperature conditions. The theoretical values of the contact stress obtained from equations appended in Appendix are given in Fig. 9.

From this experimental study, it is noticed that there is greater advantage in increasing the face width of high-helix-angle gears than using low-helix-angle gears of large face width. Assuming that the transmitted load is shared by all contacting points, it is seen from Fig. 10 that the effective contact stress reduces by almost 60 percent if the helix angle is increased from 5 deg to 45 deg, keeping the face width equal to 500 mm. Thus, although this photoelastic investigation confirms the fact that the circular-arc gear teeth are weaker at higher helix angles, higher load-carrying capacity can be obtained by increasing the helical-overlap ratio, keeping in view the allowable axial space in the respective application.

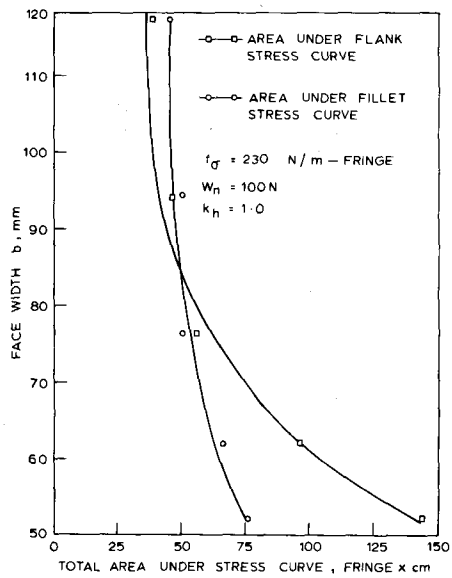

Fig. 7—Influence of face width and helix angle on the relative load-carrying capacity

Conclusions

It is concluded from this investigation that three-dimensional photoelasticity can be conveniently used to study the contact- and bending-stress distribution in circular-arc gear teeth, which by theoretical methods would involve too many assumptions and approximations.

It is concluded that there is more uniform distribution of load in lower helix angle gears, if center distance and shaft parallelism are maintained to close tolerances. Higher bending stresses are induced in high-helix-angle gears due to local deflections.

Though high-helix-angle gears have a higher contact and bending stress, load-carrying capacity of high-helix-angle gears can be increased by increasing the face width. Thus a trade-off between the load-carrying capacity and face width can be made to suit automotive applications.

Acknowledgments

The authors express their gratitude to the Bangalore University and the Council of Scientific and Industrial Research, New Delhi, which rendered financial assistance for this project.

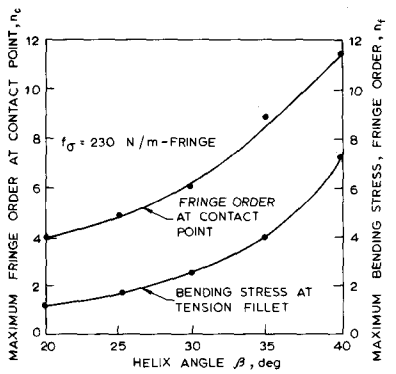

Fig. 8—Contact and bending-stress variation with helix angle

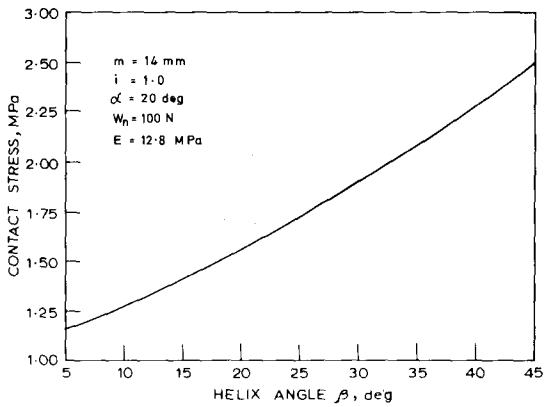

Fig. 9—Theoretical values of contact stress

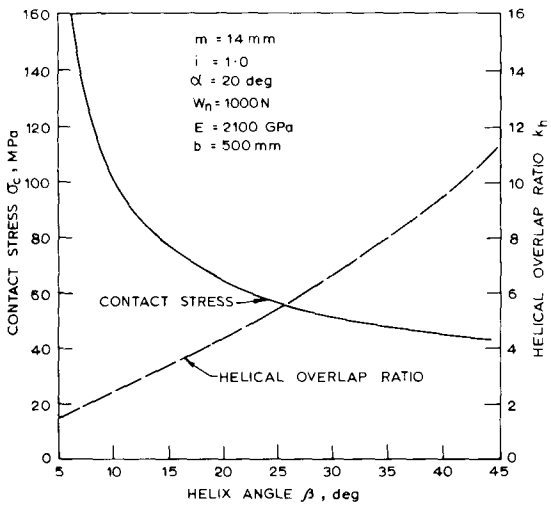

Fig. 10—Influence of k_h on contact stress

References

1. Allan, T., "Some Aspects of the Design and Performance of Wildhaber-Novikov Gearing," Proc. Inst. Mech. Engrs., 179, Part I (1964-1965).

2. Walker, H., "A Critical Look at the Novikov Gear," The Engineer, London, 209, 725-729 (Apr. 1960).

3. Johnson, D.C., "Novikov Gears: Gear Teeth with Circular Arc Profiles," Engineering, (293), (Oct. 1959).

4. Ramachandra, K. and Lingaiah, K., "Photoelastic Investigation of the Load-Carrying Capacity of Wildhaber-Novikov Circular Arc Gears," J. Inst. Engrs. (India), 53, Part ME6, 313-321 (Jul. 1974).

5. Lingaiah, K. and Ramachandra, K., "Photoelastic Optimization of the Profiles of Wildhaber-Novikov Gears," EXPERIMENTAL MECHANICS, *16 (3), 116-120 (Mar. 1976).*

6. Klein, G.J., "The Wildhaber-Novikov System of Gearing," DME/NAE Quart. Bull. (1965-1), Nat. Res. Council of Canada, Ottawa (Apr. 1965).

7. Wells, C.F. and Shotters, B.A., "The Development or Circarc Gearing," AEI Engrg, 83-88 (Mar.-Apr. 1962).

8. Dobrovolsky, V., et al., "Fundamentals of the Theory and Operation of Novikov Gears," Machine Elements, MIR Publishers, Moscow (1968).

9. Chironis, N.P., "Design of Novikov Gears," Product Engrg., 91-102 (Sept. 1962).

10. Davies, W.J., "Novikov Gearing," Machinery, 96 (4), 64-73 (Jan. 1960).

11. Lingaiah, K. and Ramachandra, K., "Technology Transfer in the Design and Development of Wildhaber-Novikov Gears," Proc. Design Tech. Transfer Conf., ASME (Apr. 1974).

APPENDIX

The maximum contact stress at the center of the contact surface[11] is given by the equations,

$$\sigma_c = \left[\frac{3W_n}{2\pi a' b'}\right] \tag{A1}$$

$$a' = x\left[\frac{1.5\pi W_n k}{\epsilon_1}\right]^{0.33} \tag{A2}$$

$$b' = y\left[\frac{1.5\pi W_n k}{\epsilon_1}\right]^{0.33} \tag{A3}$$

$$k = \frac{(1-\nu^2)}{E} \tag{A4}$$

Constants x and y in eqs (A2) and (A3) depend upon the angle θ given by

$$\theta = \cos^{-1}\left[\frac{\epsilon_2}{\epsilon_1}\right] \tag{A5}$$

ϵ_1 and ϵ_2 in eqs (A2), (A3) and (A5) are given by the following equations:

$$\epsilon_1 = \frac{1}{2m}\left[C_e\left(1 + \frac{\lambda\sin\alpha}{\phi}\right) + \frac{2z_e\lambda}{\phi}\right] \tag{A6}$$

$$\epsilon_2 = \frac{1}{2m}\left[\frac{z_1\phi - (2C_1 + z_1\sin\alpha)\lambda}{C_1 z_1 \phi} - \frac{z_2\phi + \lambda(2C_2 - z_2\sin\alpha)}{C_2 z_2 \phi}\right] \tag{A7}$$

The constants in eqs (A6) and (A7) are defined as follows:

$$C_1 = \frac{\varrho_1}{m}$$

$$C_2 = \frac{\varrho_2}{m}$$

$$C_e = \frac{C_2 - C_1}{C_2 C_1}$$

$$z_e = \frac{z_1 + z_2}{z_1 z_2}$$

$$\lambda = \tan^2\beta\sin\alpha$$

$$\phi = (1 + \tan\beta\cos\alpha)^{1.5}$$